Modeling of Aperture Fields for Cavities Excited by Stochastic Current Sources

Michael Haider, Biljana P. Stošić, Mohd H. Baharuddin,
Nebojša S. Dončov, David W. P. Thomas, Peter Russer, Johannes A. Russer

***Abstract*—Stochastic electromagnetic fields can be described by correlation spectra. In this paper, we describe modeling of the aperture field for a cavity with multiple stochastic sources for field excitation within the cavity with an arbitrary degree of correlation between the sources. In this modeling approach, the contribution to the aperture field from each radiation source is characterized experimentally and numerically by determining S-parameters first. It is shown that a variable degree of source correlation can have a significant impact on the aperture field.**

***Index Terms*—Stochastic electromagnetic fields, electromagnetic interference, electromagnetic compatibility, cavity aperture, correlation spectra, noise electromagnetic fields.**

I. Introduction

Analysis and prediction of the electromagnetic (EM) emissions from complex devices under test into the environment can be done by using results of near-field scanning. For stochastic electromagnetic fields, unlike for deterministic fields, the correlation between the EM field sources has to be considered for characterization of the field and in modeling of the field propagation [1], [2]. Radiated electromagnetic interference (EMI) and electromagnetic compatibility (EMC) are critical in design considerations for modern high performance electronics [3], [4]. Experimental characterization of devices requires near-field scanning [5]–[7]. Field correlations can be characterized with multi-channel time-domain measurement equipment with a minimum of two field probes [1], [8]–[10]. The determined correlation information serves to compute the propagation of the stochastic EM field numerically [2], [11], [12] and can also be used for source localization [13], [14]. Principal component analysis can be applied for a compact representation of correlation matrices [15].

In this work, measurements and numerical modeling of the EM field generated by several monopole antennas inside a metal enclosure, forming a cavity with one square aperture, is carried out and investigated for excitation by stochastic antenna source currents. We consider stationary stochastic sources with Gaussian probability distribution for the signals. The numerical model was created, such that it corresponds to the experimental setup used for measurements in an anechoic chamber. The excitation currents on the monopole antennas inside the enclosure can be correlated, partially correlated or uncorrelated. Characterization of a stochastic EM field requires the sampling of the tangential EM field in observation points defined on an enclosing surface and, subsequently, the determination of the cross-correlations between the field at all sampling points.

The objective of this paper is to numerically study a case relevant to EMC in order to characterize the distribution of deterministic and stochastic EM fields in the near-field and furthermore, to facilitate an efficient prediction of the field propagation into the far-field. Therefore, we use a combination of the full wave transmission line matrix (TLM) method and a network oriented correlation matrix approach [16], [17]. In addition, we obtained experimental data by frequency domain measurements using a vector network analyzer (VNA) in an anechoic chamber together with a near-field scanner. We consider the case of two monopol antennas in the cavity. Different configurations for the monopole antenna excitation are investigated, i.e. only one or both antennas excited, in order to study how the level of correlation between the sources will affect the EM field distribution on the aperture. In addition, the influence of the level of correlation between the monopole sources on the spectral energy density of the EM field in the scanning plane is investigated numerically.

In Section II, we describe the propagation of correlation information using S-parameters. We can define microwave ports for each observation point of the tangential EM field, one port for each polarization. If all S-parameters of these ports, resolved in terms of a discrete set of observation points, are known, we obtain a network based model which can be used to describe both, deterministic and stochastic field problems. We also give a detailed description of the measurement setup for the cavity with excited monopoles, we used in order to sample the aperture fields. The experimental data obtained will be compared to data from full-wave numerical EM analysis. With this data we can describe the aperture field for arbitrary source correlations, as we will discuss subsequently.

II. S-Parameter Description

Linear passive distributed microwave circuits can be described by S-parameters [18]–[20]. We consider a cavity with multiple sources exciting EM fields. The sources can be represented by N antennas distributed within the cavity. The tangential components of the aperture field can be sampled by an array of M near-field probes or by a single near-field probe which is sequentially moved to M sampling points. If the field distribution is known on the aperture, the field outside the cavity can be determined according to uniqueness theorem for deterministic sources. Also the evolution of the spectral energy

Michael Haider, Peter Russer and Johannes A. Russer are with the Institute for Nanoelectronics, Technical University of Munich, Munich, Germany, E-Mails: michael.haider@tum.de, russer@tum.de, jrusser@tum.de

Biljana P. Stošić and Nebojša S. Dončov are with the Faculty of Electronic Engineering, University of Niš, Niš, Serbia, E-Mails: biljana.stosic@elfak.ni.ac.rs, nebojsa.doncov@elfak.ni.ac.rs

Mohd H. Baharuddin and David W. P. Thomas are with the University of Nottingham, School of Electrical and Electronic Engineering, Nottingham, United Kingdom, E-Mails: mohd.baharuddin@nottingham.ac.uk, dave.thomas@nottingham.ac.uk

density for stochastic fields propagating out of the aperture can be modeled [2]. The passive structure, including source and near-field probing antennas, can be modeled by a distributed microwave circuit, where each antenna feed represents one port. At each port, an incident power wave a and a reflected power wave b can be defined. The power waves are related to the port's current I and voltage V by

$$I_n = \frac{1}{\sqrt{Z_0}} \left(a_n - b_n\right) , \tag{1a}$$

$$V_n = \sqrt{Z_0} \left(a_n + b_n\right) , \tag{1b}$$

where Z_0 is the reference impedance and the index n refers to the port number. Incident and reflected power waves can be summarized in the vectors $\mathbf{a}$ and $\mathbf{b}$

$$\mathbf{a} = \left[a_1 \dots a_N \, a_{N+1} \dots a_{N+M}\right]^T , \tag{2a}$$

$$\mathbf{b} = \left[b_1 \dots b_N \, b_{N+1} \dots b_{N+M}\right]^T , \tag{2b}$$

where ^{T} denotes the transpose vector. Both, incident and reflected power waves are related to each other via the scattering matrix $\mathbf{S}$

$$\mathbf{b} = \mathbf{S}\,\mathbf{a} . \tag{3}$$

With N antennas that will be connected to excitation sources and M near-field probing antennas, we can introduce submatrices as follows,

$$\boldsymbol{S} = \begin{bmatrix} \mathbf{S_{NN}} & \mathbf{S_{NM}} \\ \mathbf{S_{MN}} & \mathbf{S_{MM}} \end{bmatrix} . \tag{4}$$

Correlations between the power waves can be defined for the incident waves in the matrix $\mathbf{C_a}$ and for the reflected waves in the matrix $\mathbf{C_b}$

$$\mathbf{C_a} = \left\langle \mathbf{a}\mathbf{a}^\dagger \right\rangle , \tag{5a}$$

$$\mathbf{C_b} = \left\langle \mathbf{b}\mathbf{b}^\dagger \right\rangle . \tag{5b}$$

Here, $\langle \dots \rangle$ denotes the ensemble average and † the Hermitian conjugate. From (5a), (5b), and (3) we obtain

$$\mathbf{C_b} = \mathbf{S}\,\mathbf{C_a}\,\mathbf{S}^\dagger . \tag{6}$$

Assuming that the near-field probes scanning the field can be considered non-invasive there will be no incident power waves from these port, i.e. $a_n = 0$ for $n = N+1, \dots, N+M$. The correlation matrix obtained for the voltages at the observation ports is than obtained only from the reflected power waves at those ports as

$$\mathbf{C_{V_M}} = \left\langle \mathbf{V_M}\mathbf{V_M}^\dagger \right\rangle = Z_0 \mathbf{C_{b_M}} , \tag{7}$$

where $\mathbf{V_M} = \left[V_{N+1} \dots V_{N+M}\right]^T$ and $\mathbf{C_{b_M}} = \left\langle \mathbf{b_M}\mathbf{b_M}^\dagger \right\rangle$ with $\mathbf{b_M} = \left[b_{N+1} \dots b_{N+M}\right]^T$. Correlations of the source currents $\mathbf{I_N} = \left[I_1 \dots I_N\right]^T$ and their relation to the incident power waves at the source ports is given as

$$\mathbf{C_{I_N}} = \left\langle \mathbf{I_N}\mathbf{I_N}^\dagger \right\rangle = \frac{1}{Z_0}\Big(\mathbf{C_{a_N}} + \mathbf{S_{NN}}\mathbf{C_{a_N}}\mathbf{S_{NN}}^\dagger - \mathbf{S_{NN}}\mathbf{C_{a_N}} - \mathbf{C_{a_N}}\mathbf{S_{NN}}^\dagger\Big) , \tag{8}$$

with $\mathbf{C_{a_N}} = \left\langle \mathbf{a_N}\mathbf{a_N}^\dagger \right\rangle$ where $\mathbf{a_N} = \left[a_1 \dots a_N\right]^T$.

III. Near-Field Measurement and Modeling of Cavity Aperture

Near-field measurements are performed by sampling the tangential EM field close to the device under test (DUT) on discrete locations prescribed on an enclosing surface. In this case, a uniform rectangular grid of sampling points is chosen. In this planar near-field measurement scheme, the data acquisition requires the probe to move in two orthogonal linear directions in a rectangular coordinate systems. Near-field data are acquired on a plane which has to be finite in extent but which intercepts the major portion of the radiation field, i.e. the Poynting vector drops significantly in its magnitude outside the sampling area. The far-field pattern can be calculated from the measured near-field. Whereas a characterization of a stochastic EM field requires a two-probe measurement, the propagation of the stochastic field in a deterministic environment can be computed with the help of numerical Green's functions pertaining to the respective geometry.

To perform our experimental and numerical studies for the DUT, a near-field measurement system has been built, which includes on the hardware side the device under test, which is a cavity formed by a metal enclosure with two monopole antennas inside, a planar scanner comprised of a three-axis (x, y and z) automated system, controlling the position of a magnetic loop probe which is connected to the second channel of a vector network analyzer (VNA). The first channel is connected to either one or both monopoles inside the cavity. A personal computer is set up to run software to control the scanning system and to trigger measurements of the VNA. Subsequently, near-field measurements are performed using the near-field measurement system inside an anechoic chamber. In the following, we will consider only a single component of the tangential field. The acquired experimental data is further post-processed. A model of the DUT was established in CST, a commercially available state-of-the-art numerical full-wave EM analysis tool. The results obtained from the numerical model of the DUT is validated by comparing them with experimental results obtained by measurements inside an anechoic chamber. Finally, different scenarios are investigated to assess how the degree of correlation between the sources affects the EM field distribution on the aperture.

A. Measurement Setup

The sampling of noisy EM field in the near-field above a DUT is conducted in an anechoic chamber. The metal enclosure with two monopole antennas serving as DUT is depicted in Fig. 1(a). The internal dimensions of the cavity are $(216 \times 180 \times 252)$ mm^3. The dimensions of the removable enclosure lid (in yz-plane) with one square aperture, are extended on both sides in z- and y-directions by 18 mm from the edges of enclosure. The thickness of the cavity walls, made from brass sheet with 10 Ohm/sq, is 1 mm. The size of the aperture is (108x108) mm^2, symmetrically positioned in y-direction (at a distance of 54 mm from the lid's edges) and asymmetrically positioned in z-direction (at a distance of 108 mm from one and at distance of 72 mm from the other edge of the lid), as shown in Fig. 1(b).

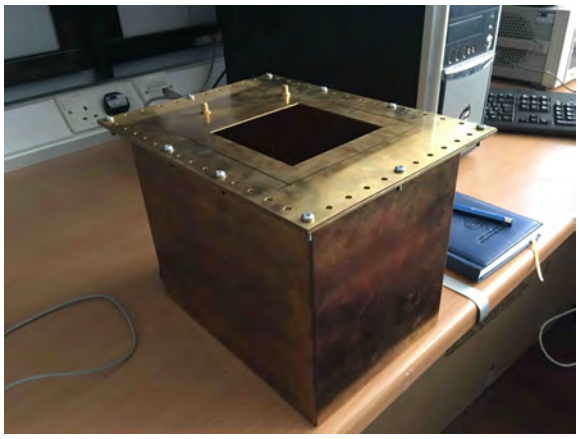

(a) An enclosure with removable lid.

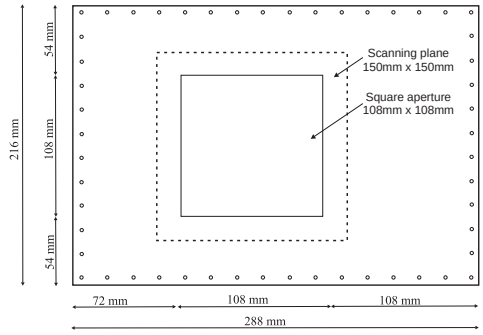

(b) The removable enclosure lid with one square aperture.

Fig. 1. An enclosure used in measurements.

(a) RF loop probe.

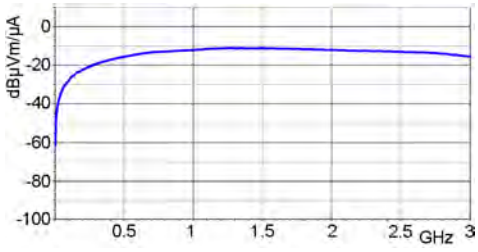

(b) Frequency characteristic of RF probe used in measurements.

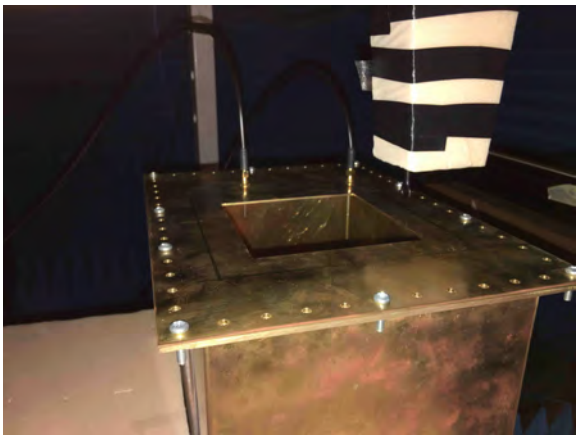

(c) Experimental enclosure with RF loop probe placed above the removable enclosure lid.

Fig. 2. An enclosure with RF loop probe.

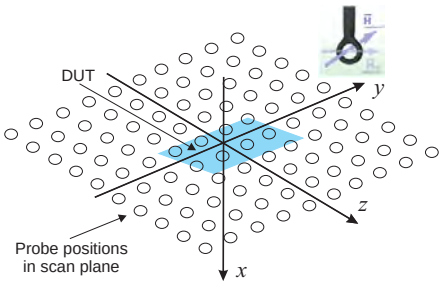

Fig. 3. Near-fied probe positions.

The monopole antennas inside the cavity are attached to the removable enclosure lid and they are of 27 mm lengths and 0.5 mm radius. The position of the monopole closer to the apertures (monopole 1) is offset by 9 mm in y- and 27 mm in z-direction from the lower right corner of the aperture as of Fig. 1(b), while the second monopole (monopole 2) is offset by 81 mm in y- and 45 mm in z-direction.

The magnetic field component in y-direction of the aperture field excited by the monopole antennas is measured by a loop probe RF-R 50-1 (Langer EMV-Technik GmbH) shown in Fig. 2(a), scanning at a distance of 10 mm above the removable enclosure lid. The scanning plane is of (150×150) mm^2 size and it is symmetrically positioned above one square aperture. It is divided into (31x31) points uniformly spaced with 5 mm separation. The RF loop probe is positioned in each point using LabVIEW software to control the positioning system (see Fig. 3). One channel of the VNA was used to excite either one of the two monopole antennas separately or both antennas at the same time using a power splitter, while the other channel was connected to the RF loop probe (Fig. 4).

B. Measurement and Numerical Modeling Results

The following cases were considered experimentally and numerically: (1) only monopole 1 is excited, (2) only monopole 2 is excited and (3) both monopole antennas are excited at the same time using a power splitter. The aperture field is scanned for all these cases and S-parameters are determined.

Measurement results for the obtained S-parameters are shown in Fig. 5 for the frequency $f = 1$ GHz. The absolute value of S_{21} is ploted, where port '1' is the input port to either one or both (via power splitter) of the monopol antennas, and port '2' is the near-field probe for which the position is being varied. Here, different from the description in the previous section, we keep the index '2' for the ports of the aperture field while the sampling points actually cover positions $N+1$ to M. The obtained plots are compared to the magnitude of the y-component of the H-field, as obtained by numerical full wave simulation using the TLM solver of CST. The S-parameter plots, closely related to the H-field plots show, as expected, qualitatively very good agreement. S-parameter data can also be obtained straight forward from the numerical model. Using S parameters obtained for each single source excitation allows to set up a model to describe the aperture field under excitation by partially correlated fields as described above.

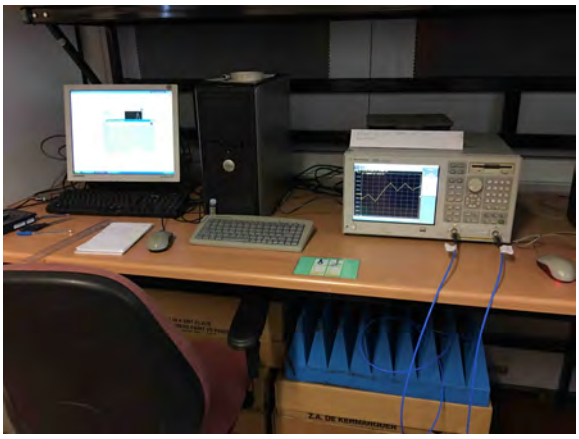

Fig. 4. Experimental set-up (PC with LabVIEW and VNA).

C. Modeling of Excitation by Stochastic Sources

As described in Section II, correlations of power waves can be given with the help of S-parameters. The spectral energy density (SED) of the stochastic EM field is directly proportional to the autocorrelation functions of the electric or magnetic field components [2]. In Fig. 6, we have given plots for the aperture field for excitations by the two monopoles with varying degree of source correlations. Plots show the field for monopole excitation with uncorrelated sources (Fig. 6(a)), correlated in phase (Fig. 6(b)), and correlated anti-phase (Fig. 6(c)), all at $f = 1$ GHz. For the anti-phase excitation, energy levels are very low in the aperture, and they peak for in-phase excitation. Levels lie in between for an uncorrelated excitation. Plots in Figs. 6(d)-(h) show the energy in the aperture field for $f = 2$ GHz. Here, field patterns are more distinct for the excitation of the different monopoles. Variable degree of source correlations are shown and their impact on the resulting aperture field is illustrated by the SED plots.

The measurements carried out as well as the numerical results will contribute to the further development of the methodology for characterizing stochastic EMI sources in the near-field and to account for propagation of radiated EMI in either open or closed, densely integrated environments by using computationally efficient numerical tools.

IV. Conclusion

We described modeling of the aperture field for a cavity containing multiple sources. The field excitation within the cavity stems from stochastic sources with an arbitrary degree of correlation between them. The contribution to the aperture field from each radiation source was characterized experimentally and numerically for a specific example by determining S-parameters. Variable degree of source correlation was considered in the subsequent modeling and the impact on the aperture field was shown.

V. Acknowledgment

This work was supported by the European Union's Horizon 2020 research and innovation programme under grant no. 664828 (NEMF21), by COST Action IC1407, by the Deutscher Akademischer Austauschdienst (DAAD), and by the Ministry for Education, Science and Technological Development of Serbia under the project TR-32052.

References

[1] J. A. Russer and P. Russer, "An efficient method for computer aided analysis of noisy electromagnetic fields," in *2011 IEEE MTT-S Int. Microwave Symp. (IMS)*. IEEE, Jun. 2011, pp. 1–4.

[2] ——, "Modeling of noisy EM field propagation using correlation information," *IEEE Transactions on Microwave Theory and Techniques*, vol. 63, no. 1, pp. 76 – 89, Jan. 2015.

[3] E. P. Li, X. C. Wei, A. C. Cangellaris, E. X. Liu, Y. J. Zhang, M. D'Amore, J. Kim, and T. Sudo, "Progress review of electromagnetic compatibility analysis technologies for packages, printed circuit boards, and novel interconnects," *IEEE Transactions on Electromagnetic Compatibility*, vol. 52, no. 2, pp. 248–265, May 2010.

[4] C. R. Paul, *Introduction to Electromagnetic Compatibility*. Hoboken, NJ: Wiley, 2006.

[5] A. Tankielun, U. Keller, E. Sicard, P. Kralicek, and B. Vrignon, "Electromagnetic Near-Field scanning for microelectronic test chip investigation," *IEEE EMC Society Newsletter (October 2006)*, 2006.

[6] X. Tong, D. Thomas, A. Nothofer, P. Sewell, and C. Christopoulos, "Modeling electromagnetic emissions from printed circuit boards in closed environments using equivalent dipoles," *IEEE Transactions on Electromagnetic Compatibility*, vol. 52, no. 2, pp. 462–470, May 2010.

[7] C. Smartt, D. Thomas, H. Nasser, M. Baharuddin, G. Gradoni, S. Creagh, and G. Tanner, "Challenges of time domain measurement of field-field correlation for complex PCBs," in *Electromagnetic Compatibility (EMC), 2015 IEEE International Symposium on*, Aug 2015, pp. 953–958.

[8] J. A. Russer, N. Uddin, A. S. Awny, A. Thiede, and P. Russer, "Near-field measurement of stochastic electromagnetic fields," *Electromagnetic Compatibility Magazine, IEEE*, vol. 4, no. 3, pp. 79–85, 2015.

[9] J. A. Russer, M. Haider, M. H. Baharuddin, C. Smartt, A. Baev, S. Wane, D. Bajon, Y. Kuznetsov, D. Thomas, and P. Russer, "Correlation measurement and evaluation of stochastic electromagnetic field," in *Proc. EMC Europe*, Wroclaw, Poland, 2016.

[10] J. A. Russer, M. Haider, M. H. Baharuddin, C. Smartt, S. Wane, D. Bajon, A. Baev, Y. Kuznetsov, D. Thomas, and P. Russer, "Near-field correlation measurement and evaluation of stationary and cyclostationary stochastic electromagnetic fields," in *Proc. European Microwave Conference (EuMC)*. London, U.K.: IEEE, October 3-7 2016.

[11] G. Gradoni, S. C. Creagh, G. Tanner, C. Smartt, and D. W. P. Thomas, "A phase-space approach for propagating field-field correlation functions," *New Journal of Physics*, vol. 17, no. 9, p. 093027, 2015.

[12] J. A. Russer, A. Cangellaris, and P. Russer, "Correlation transmission line matrix (CTLM) modeling of stochastic electromagnetic fields," in *2016 IEEE MTT-S Int. Microwave Symp. (IMS)*, May 2016, pp. 1–4.

[13] A. Gorbunova, A. Baev, M. Konovalyuk, Y. Kuznetsov, and J. A. Russer, "Stochastic EMI sources localization algorithm based on time domain planar near-field scanning," in *Electromagnetic Compatibility (EMC EUROPE), 2013 International Symposium on*. IEEE, September 2013, pp. 972–976.

[14] Y. Kuznetsov, A. Baev, A. Gorbunova, M. Konovalyuk, D. Thomas, C. Smartt, M. H. Baharuddin, J. A. Russer, and P. Russer, "Localization of the equivalent sources on the PCB surface by using ultra- wideband time domain near-field measurements," in *Proc. EMC Europe*, Wroclaw, Poland, 2016.

[15] M. Haider and J. A. Russer, "Principal component analysis for efficient characterization of stochastic electromagnetic fields," *International Journal of Numerical Modelling: Electronic Networks, Devices and Fields*, 2017, accepted for publication.

[16] C. Christopoulos, *The Transmission-Line Modeling Method TLM*. New York, NY: IEEE Press, 1995.

[17] P. Russer and J. A. Russer, "Some remarks on the transmission line matrix (TLM) method and its application to transient EM fields and to EMC problems," in *Computational Electromagnetics—Retrospective and Outlook*, I. Ahmed and Z. D. Chen, Eds. Heidelberg: Springer, August 28 2014, pp. 29–56.

[18] P. Russer, *Electromagnetics, Microwave Circuit and Antenna Design for Communications Engineering*, 2nd ed. Boston: Artech House, 2006.

[19] S. Ramo, J. R. Whinnery, and T. van Duzer, *Fields and Waves in Communication Electronics*, 3rd ed. New York: John Wiley, Feb. 1994.

[20] J. A. Russer, Y. Kuznetsov, and P. Russer, "Discrete-time network and state equation methods applied to computational electromagnetics," *Mikrotalasna Revija (Microwave Review)*, pp. 2–14, July 2010.

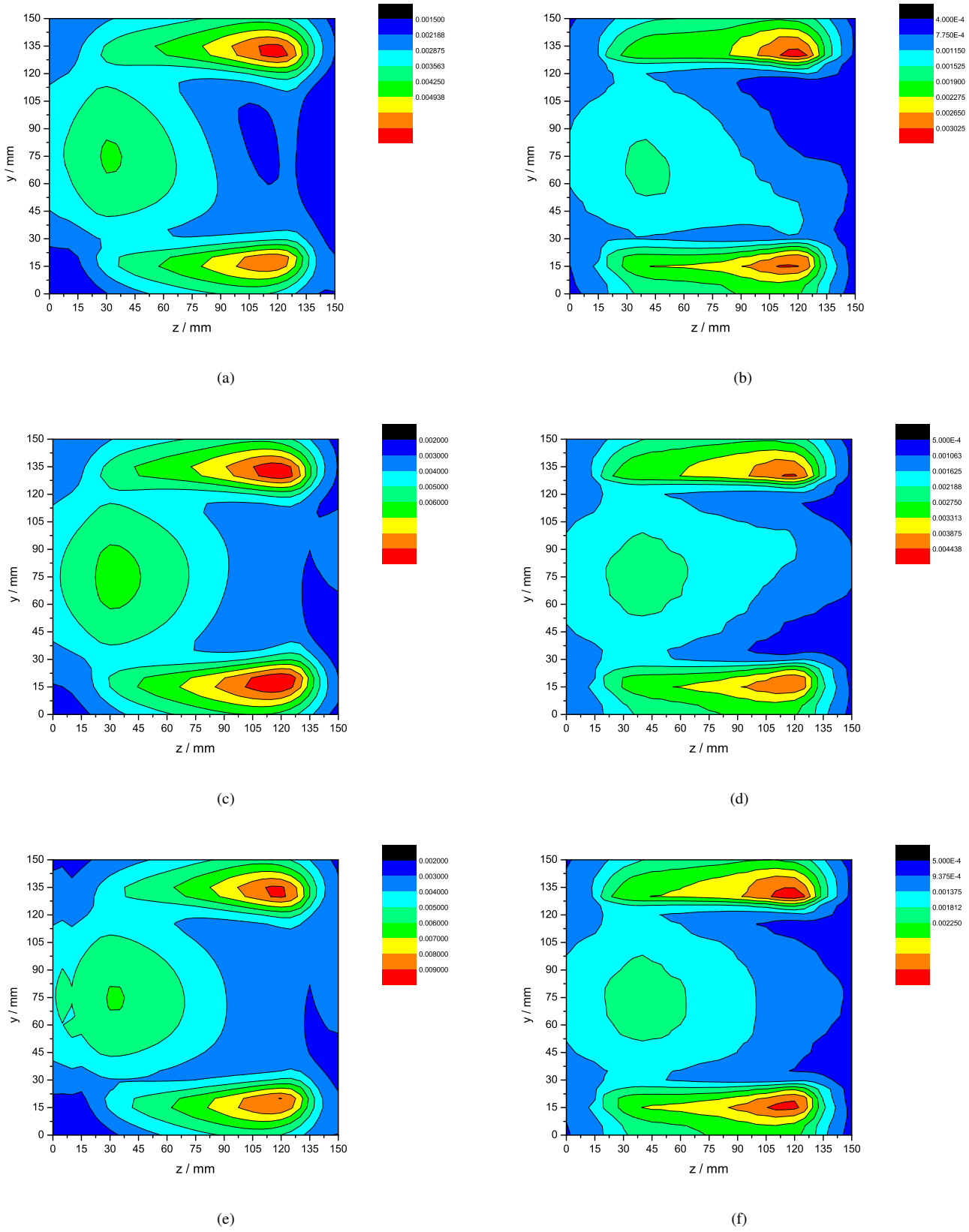

Fig. 5. Monopole 1 excited a) $|S_{21}|$ from measurement, b) $|H_y|$ from simulation; monopole 2 excited c) $|S_{21}|$ from measurement, d) $|H_y|$ from simulation; and both monopoles excited e) $|S_{21}|$ from measurement, f) $|H_y|$ from simulation; (all for $f = 1$ GHz,)

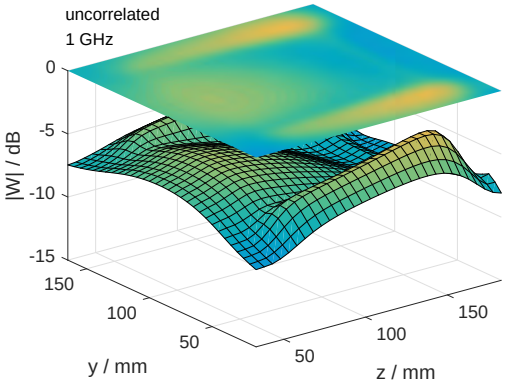

(a) SED due to excitation by two uncorrelated sources.

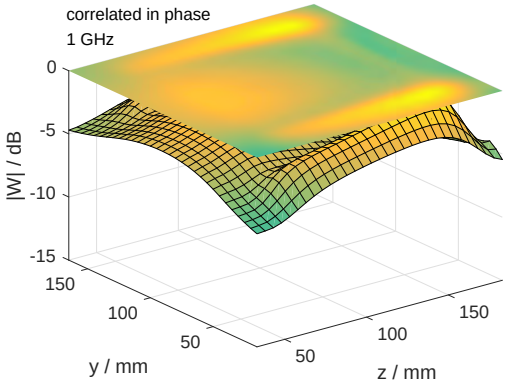

(b) SED due to excitation by two correlated sources in phase.

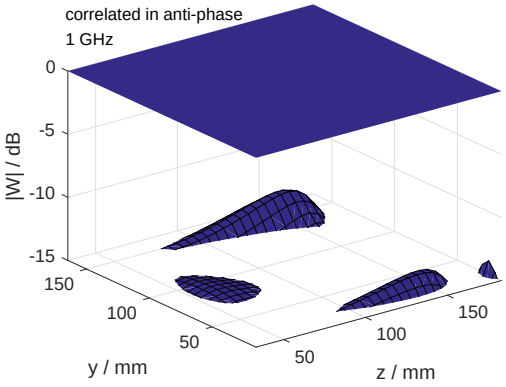

(c) SED due to excitation by two correlated sources in anti-phase.

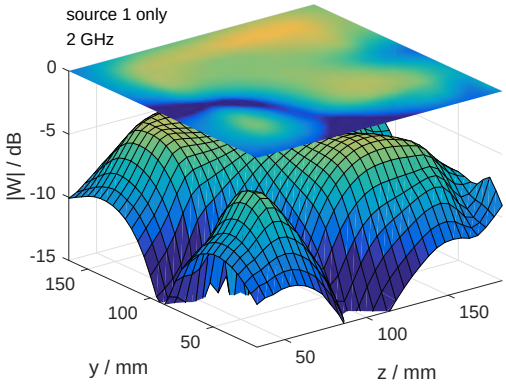

(d) SED due to excitation by source 1 only.

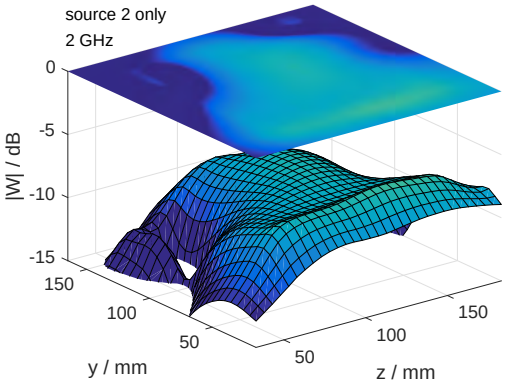

(e) SED due to excitation by source 2 only.

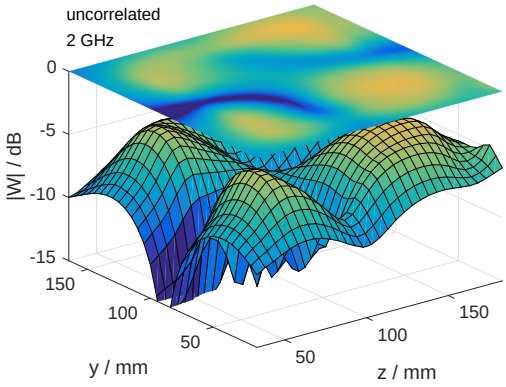

(f) SED due to excitation by two uncorrelated sources.

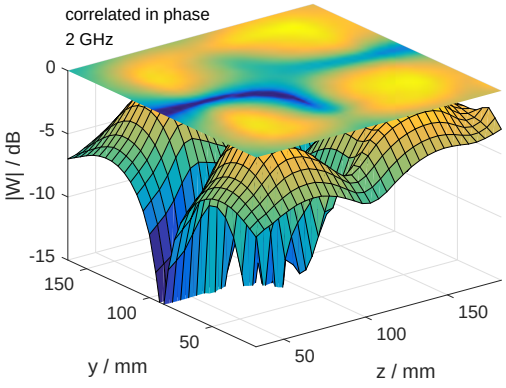

(g) SED due to excitation by two correlated sources in phase.

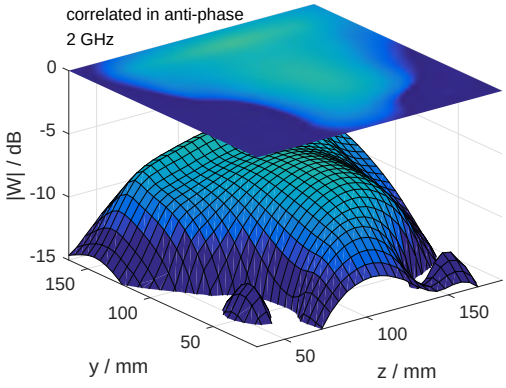

(h) SED due to excitation by two correlated sources in anti-phase.

Fig. 6. Spectral energy density (SED) at the aperture due to various excitations for $f = 1$ GHz (a)-(c) and $f = 2$ GHz (d)-(h).